Hydrogen bonding in amorphous silicon with use of the low-pressure chemical-vapor-deposition technique

G. Amato
Istituto Elettrotecnico Nazionale Galileo Ferraris, Strada delle Cacce 91, I-10135 Turin, Italy

G. Della Mea
Dipartimento Ingegneria dei Materiali, University of Trento, Trento, Italy

F. Fizzotti, C. Manfredotti, and R. Marchisio
Dipartimento Fisica Sperimentale, University of Turin, via P. Giuria 1, I-10125 Turin, Italy

A. Paccagnella
Unitá INFM, Dipartimento di Elettronica e Informatica, University of Padua, via Gradenigo 6a, I-35131 Padua, Italy
(Received 20 March 1990; revised manuscript received 23 October 1990)

Infrared spectroscopy, elastic-recoil detection analysis (ERDA), and hydrogen evolution have been used to carefully determine the hydrogen content of low-pressure chemically-vapor-deposited *a*-Si:H films. The amount of hydrogen and the bonding character can be easily varied by changing the deposition conditions. The stretching peaks at $\sim$2000 and $\sim$2100 cm^{-1} have been deconvoluted and the integrals calibrated by means of ERDA. The results provide the exact calibration constants for both peaks, and the values for the dipole effective charge obtained so far are consistent with the theory. Hydrogen-effusion measurements show that it is fairly certain that the material presents a small amount of voids, if compared with plasma-deposited amorphous silicon, despite the fact that the $\sim$2100-cm^{-1} peak can be detected in vibrational spectra. This result seems to confirm that the character of hydrogen bonding is not related to the amount of voids in the material. On the other hand, no presence of microcrystallites is detectable in Raman spectra and the sample quality, tested by means of photothermal-deflection spectroscopy, does not seem to depend on the relative strengths of the two stretching modes.

INTRODUCTION

The effect of incorporation of hydrogen in amorphous semiconductors allows us to steeply improve the electronical and optical properties of the films.[1] One of the most direct identifications of the local environment of H atoms in an *a*-Si matrix is obtained by means of infrared vibrational spectra. These spectra commonly exhibit a stretching doublet at $\sim$2000 and $\sim$2100 cm^{-1},[2] but some other structures are present.[2,3]

The wagging-rocking-rolling (640 cm^{-1}) and bending (890 cm^{-1}, 860 cm^{-1}) modes have been used to calculate the hydrogen content in the film,[3] but, in some cases, they are difficult to detect. Thus, the stretching doublet seems to provide more reliable results.

Very comprehensive studies of the vibrational spectra of *a*-Si:H have been carried out in the past.[2-4]

On the other hand, the assignment of the $\sim$2100-cm^{-1} mode has been the subject of a long-standing controversy. It is generally accepted that this mode is correlated with the presence of SiH_2, $(SiH_2)_n$, or SiH_3 configurations. Nevertheless, the possibility that the $\sim$2100-cm^{-1} structure arises from interacting Si—H bonds on the inner surface of microvoids has been suggested.[5] Recent publications[6-10] associate the $\sim$2100-cm^{-1} mode with poor photoelectronic properties of the material.

The question concerning the assignment of the $\sim$2100-cm^{-1} mode and its association with low material quality still remains unsolved: in a recent work,[11] various arguments that do not confirm these two explanations have been provided, and the need of further study has been pointed out.

Low-pressure chemically-vapor-deposited (LPCVD) *a*-Si:H has gained less attention than plasma-enhanced chemically-vapor-deposited (PECVD) or sputtering one, the most likely reason being the low hydrogen content detected in the films which have been grown in the past.[12]

In recent years, a great deal of effort has gone into[13,14] improving the photoelectronic properties of LPCVD *a*-Si:H: the results are encouraging in view of a possible application in the photovoltaic field.

Furthermore, the relative unsensitivity of the material to degradation phenomena (Staebler-Wronski effect) has been pointed out.[15]

In Fig. 1, a photothermal-deflection-spectroscopy (PDS) spectrum as obtained on a typical good-quality LPCVD sample (sample 15 in Table I), is reported. The Urbach's tail slope is 65 meV while the density of states as estimated by means of the deconvolution of the absorption spectrum in the low-energy range is $\sim 2\times 10^{16}$ cm^{-3}.

The dark conductivity has been evaluated to be $\sigma_d \simeq 10^{-9}$ $(\Omega\,cm)^{-1}$ and the photoconductivity in AM1

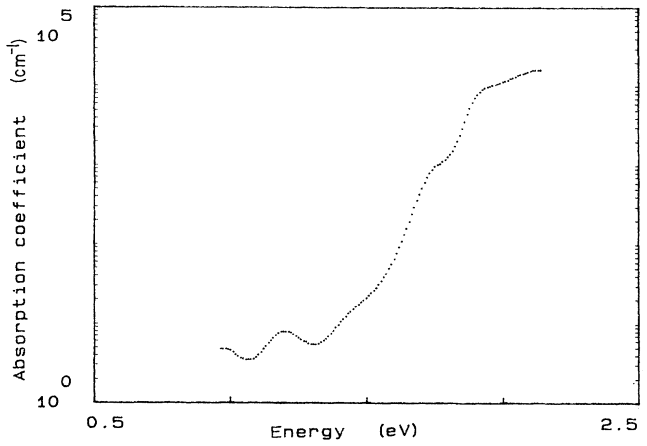

FIG. 1. The absorption coefficient spectrum as obtained by PDS on a good-quality LPCVD *a*-Si:H film.

(air mass 1) conditions is $\sigma_L \simeq 10^{-4}\,(\Omega\,\mathrm{cm})^{-1}$.

This means that the best LPCVD films, even if not comparable with the best PECVD ones, can show good photoelectronic properties, typical of the material deposited a few year ago by means of plasma reactions. The main difference between these two classes of film is that the temperature involved in the LPCVD process ($T_d > 400\,^\circ\mathrm{C}$) is much higher and the ion bombardment is absent.

Thus, an accurate study of the vibrational spectra of LPCVD *a*-Si:H seems to be necessary: it can provide useful information either for the improvement of the LPCVD technique, or for a better understanding of the unsolved problems related to the hydrogen bonding in *a*-Si:H films.

The aim of this work is to compare ir spectroscopy with elastic-recoil-detection analysis (ERDA) and hydrogen effusion, in order to obtain the effective dipole charges for the ~2000- and ~2100-cm^{-1} modes and to discuss the correlation between the presence of the ~2100-cm^{-1} peak and the structural properties of the LPCVD material.

EXPERIMENT

Films of *a*-Si:H have been grown through thermal decomposition of Si_2H_6 in a 2-m-long quartz reactor.

The deposition parameters useful to control the growth kinetics are pressure, temperature, and gas flux. Among them the first two have been chosen, in the attempt of tuning the film hydrogen content and bonding coordination. The temperature range was 400 °C–450 °C, while pressure was in the 1–10-mTorr interval.

⟨111⟩ silicon wafers have been chosen as substrates for both ir and ERDA measurements. Quartz or Corning glass substrates have been used in some cases for the ERDA analysis. In these cases, the substrate in the growth tube was placed close to a crystalline silicon wafer used for ir measurements.

Samples grown on quartz were used for hydrogen-effusion process.

A FFT Perkin Elmer spectrometer was used for ir spectroscopy. The principle behind ERDA (Ref. 16) is quite simple, being the technique similar to ion backscattering. A beam of ions with mass M_1 (^{4}He in our case) greater than that of atoms to be profiled (^{1}H) and energy E_{in} of the order of 1 MeV/amu is incident on a sample tilted at an angle $\phi = 75°$. The incident beam undergoes elastic collisions with atoms in the target while it decelerates along its trajectory according to the stopping power of the sample. The recoiled H ions exit with an energy $E_{\mathrm{out}} < E_{\mathrm{in}}$, and can be detected by a silicon surface-barrier detector covered by a slit and a thin foil. The aperture is used for the definition of the scattering angle and the foil acts as a particle filter, by stopping the incident ^{4}He ions elastically recoiled by the target in the

TABLE I. The summary of the experimental results as obtained on several samples (not available data are indicated with n.a.).

Sample	Thickness (μm)	Si—H (at. %)	Si—H_2 (at. %)	ω_t(2000) (cm^{-1})	ω_t(2100) (cm^{-1})	ERDA (at. %)
1	0.48	1.96	3.89	1996	2069	4.8
2	0.4	2.57	3.53	1994	2067	5.8
3	0.3	3.31	3.27	1991	2063	7
4	0.23	3.94	1.63	1989	2055	5.4
5	0.3	4.02	2.31	1993	2068	6.3
6	0.27	3.54	1.5	1990	2063	5.1
7	0.21	3.45	1.35	1988	2055	4.2
8	1.04	1.9	<0.2	1991	2070	2.1
9	1.4	1.88	<0.2	1990	2070	2.1
10	0.85	2.51	10.28	2000	2075	13
11	0.95	3.08	6.74	1996	2072	9.8
12	0.6	2.75	3.79	1993	2066	6.9
13	0.58	2.82	3.76	1994	2064	7.1
14	0.46	3.15	2.9	1991	2061	6.7
15	0.78	2.23	5.3	1990	2063	n.a.

same direction of light atoms. The detected H atoms have an energy $E_d = E_{\text{out}} - \Delta E$, where ΔE is the energy loss through the foil.

The H concentration profile can be obtained by comparing the spectrum of the analyzed sample with a suitable standard.

RESULTS AND DISCUSSION

Infrared spectra present some structures, as described above, that are sometimes difficult to separate from the interference fringes pattern. In particular, only the $\sim$2000- and $\sim$2100-cm^{-1} doublet has provided reliable results in our case.

To eliminate the interference fringes pattern, the following procedure has been used. The film refractive index has been calculated by means of the Kramers-Kronig transform of the imaginary part of the dielectric constant. This quantity has been parametrized by means of available models[17] and the parameters have been obtained by fitting the experimental data in the 1–4-eV energy range.[18]

This procedure allows us to determine the Fresnel coefficients at the air-film and film-substrate interfaces, being the substrate refractive index $n_s \simeq 3.4$

The ir transmission experimental data have been corrected for the substrate transmission and hence converted into absorption ones, by using some common relationships.[19] In this manner, the absorption spectrum without interference fringes can be obtained.

Figure 2 shows the absorption coefficient behavior in the region 1800–2300 cm^{-1} for a typical sample as obtained by means of this procedure.

The contribution of an ir-active vibration of a Si—H band of frequency ω_t to the complex transverse dielectric constant is[11]

$$\Delta\epsilon(\omega) = (4Ne_S^{*2}/\mu)/(\omega_t^2 - \omega^2 - i\gamma\omega) \ , \tag{1}$$

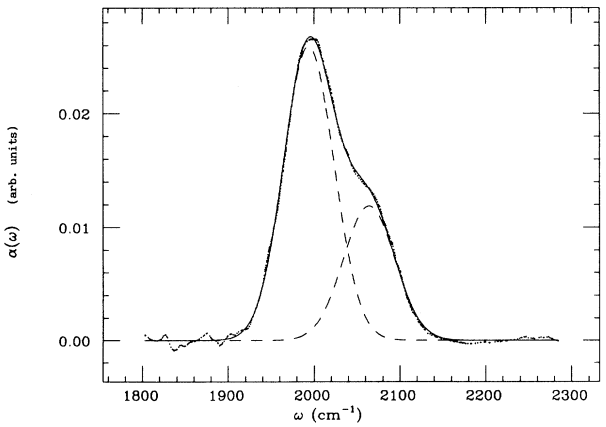

FIG. 2. The ir absorption coefficient for a typical sample obtained after suppression of the interference fringes (dotted line). Deconvoluted peaks at $\sim$2000 and $\sim$2100 cm^{-1} (dashed line). The dashed line represents the best fit of the experimental dotted line.

where

$$\omega_t^2 = \omega_0^2 - \tfrac{4}{3}\pi N e_S^{*2}/\mu \ , \tag{2a}$$

and

$$\omega_0^2 = K_0/\mu \ , \tag{2b}$$

K_0 is the restoring force constant, ω_0 the Si—H stretching frequency in the free molecule, γ is the damping constant, N the number of oscillations per unit volume, μ the reduced mass, and e_S^* the effective dipole charge.

If the separation between the peaks of the doublet in Fig. 2 is needed, an appropriate deconvolution procedure has to be applied in order to obtain two Lorentzian curves. For this purpose the minimization program MINUIT has been used, and the deconvolution result is reported in the same figure.

It is well known that by integrating the peaks in the absorption coefficient $\alpha(\omega)$ spectra, the obtained quantity is related to the H amount in the sample[2] through the equations

$$N_S = A_S I_S \ \text{cm}^{-3} \ , \tag{3a}$$

with

$$I_S = \int \omega^{-1}\alpha(\omega)d\omega \ , \tag{3b}$$

where the integral is extended to only one of the absorption modes and A_S is a constant.

Equation (3) can be rewritten in order to meet our case as

$$N_S = A_S \int_{\sim 2000\ \text{cm}^{-1}} \omega^{-1}\alpha(\omega)d\omega + B_S \int_{\sim 2100\ \text{cm}^{-1}} \omega^{-1}\alpha(\omega)d\omega \ , \tag{4}$$

where $A_S(\text{cm}^{-2})$ and $B_S(\text{cm}^{-2})$ are the calibration constants for the two modes.

Since the total H concentration has been obtained by means of ERDA measurements, a two-dimensional linear fit can be applied to experimental data, in order to evaluate A_S and B_S.

The result of the fit is shown in Fig. 3: the x axis reports the H percent calculated by means of (4) and normalized on the Si atoms concentration, while on the y axis the same quantity, evaluated by means of ERDA, is quoted. As it can be seen, the data are highly correlated and the choice of the substrate for ERDA measurements (the circles represent c-Si substrates, while the diamonds represent quartz or Corning glass substrates) does not play any role.

The values of A_S and B_S obtained so far are the following:

$$\begin{aligned} A_S(\omega \sim 2000\ \text{cm}^{-1}) &= (7.34 \pm 1.00) \times 10^{19}\ \text{cm}^{-2} \ , \\ B_S(\omega \sim 2100\ \text{cm}^{-1}) &= (2.06 \pm 0.15) \times 10^{20}\ \text{cm}^{-2} \ . \end{aligned} \tag{5}$$

These results do not agree with those reported in Ref. 2, but it will be shown by the following considerations that they are consistent with the theory.

First of all, the values of the dipole effective charges e_S^*

can be evaluated from A_S and B_S following the treatment of Ref. 2:

$$A_S = cn\mu\omega_0/(2\pi^2 e_S^{*2}) \text{ cm}^{-2} . \quad (6)$$

From this we obtain

$$e_S^*(\omega \sim 2000 \text{ cm}^{-1}) = 0.44, \; e_S^*(\omega \sim 2100 \text{ cm}^{-1}) = 0.26 . \quad (7)$$

It has been argued that a solid-state effect[2,3,5] can account for the discrepancy between the values of e_S^* in (7) and the free-molecule effective charge e_G^*. The value of e_G^* has been assessed to be $e_G^* = 0.16$. The solid-state effect consists in the presence of a local field which differs from the applied field. There are two main approaches for the local-field corrections.[4] The first is the Onsager local-field approximation, which considers a point dipole into a spherical cavity within the dielectric medium. The second approximation uses the Lorentz local field and treats the absorber as embedded in a dielectric medium. It is widely accepted that the first approximation could be more correct.[2]

The relationship between e_S^* an e_G^* can thus be written as

$$e_S^* = [3\epsilon/(1+2\epsilon)]e_G^* \quad (8)$$

where ϵ is the electronic dielectric constant of the medium.

Equation (8) gives

$$e_S^* = 0.23 \quad (9)$$

in clear agreement with the result obtained for the mode at $\sim 2100 \text{ cm}^{-1}$.

A second consideration consists in the evaluation of the frequency shift of the peaks, due to the solid-state effect. As it can be recognized in Fig. 2 and in Table I, the peaks maxima are generally centered around 1990 and 2060 cm^{-1}. A similar type of shift has been reported by other authors[3] on sputtered samples, annealed at $T > 500\,^\circ\text{C}$.

The theoretical calculation on the solid-state shift $\Delta\omega$ can be carried out, following Ref. 2: if we consider the free-molecule vibrational frequencies of the SiH band (2080 cm^{-1}) and of the SiH_2 band (2128 cm^{-1}) (as reported in Ref. 2), we obtain shift values $\Delta\omega = -88 \text{ cm}^{-1}$ and $\Delta\omega \sim -51 \text{ cm}^{-1}$, respectively. This result is in excellent agreement with the experimental evaluations.

A last consideration arises if we compare the mean value $(A_S + B_S)/2$ with the experimental calibration constant as reported by Shanks *et al.*[3] In that paper, the integrated strength I_S of the bond stretching band around 2000–2100 cm^{-1} has been related to the H concentration as measured by nuclear techniques by means of Eq. (3).

The value of A_S reported therein is $A_S = 1.4 \times 10^{20}$ cm^{-2}.

The mean value $(A_S + B_S)/2$ obtained by (5) is $(1.39 \pm 0.12)\ 10^{20}$ cm^{-2} in clear agreement with Ref. 3. As a matter of interest, no relevant changes are obtained if the same integrating procedure of Ref. 3 is followed.

At this point, a brief discussion about the structural

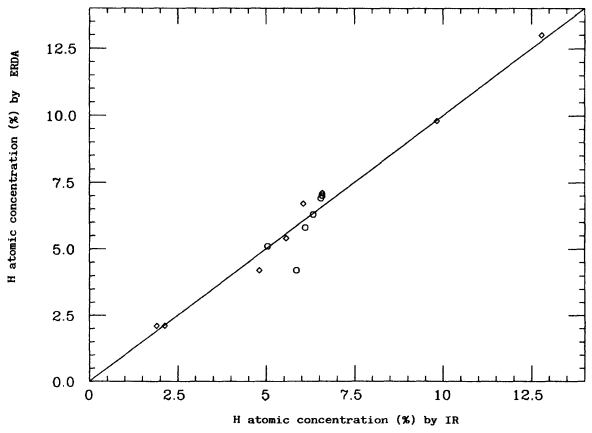

FIG. 3. The correlation between H atomic percentage obtained by means of ERDA and ir measurements. For the ir evaluation, the calibration constant values reported in the text have been used. For ERDA measurements both *c*-Si substrates (open circles) and quartz or Corning glass ones (diamonds) have been used.

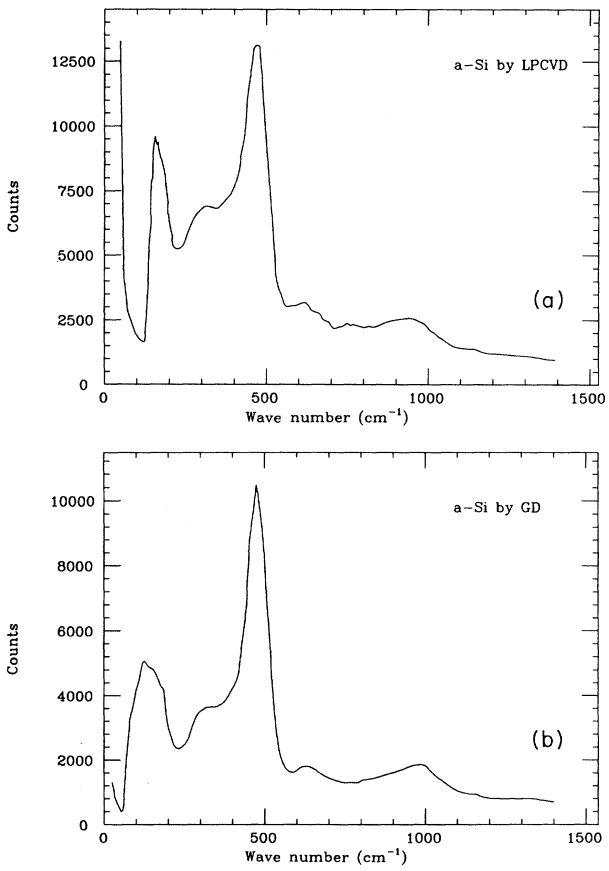

FIG. 4. Raman spectra for (a) a typical LPCVD sample compared with (b) a good-quality plasma-deposited one.

properties of LPCVD amorphous silicon seems to be necessary. In fact, as it can be seen in Table I, the percentage of SiH_2 bonds is in many cases comparable with the Si—H one, even higher in some samples. It is generally believed that by increasing the strength of the $\sim$2100-cm^{-1} mode, the quality of the films degrades.

The PDS result reported in Fig. 1 together with the photoconductivity measurements, referred to as sample 15 does not to agree with this viewpoint. In particular, the best quality samples we have obtained show a Si—H_2 bond concentration, which is approximately two or three times the Si—H bond one.

Another effect which could be correlated with the presence of the $\sim$2100-cm^{-1} mode is the degree of microcrystallinity of the film. In order to check if the microcrystallites are present, Raman spectroscopy has been used on LPCVD films and the results have been compared with those obtained in the case of good-quality plasma-deposited films. Figure 4 compares the Raman spectrum obtained on a typical LPCVD sample with that of a good-quality (defect density below 10^{16} cm^{-3}) PECVD film. It can be argued that the shape of the two spectra is essentially the same. The peaks of the TO phonon at $\sim$470 cm^{-1} have essentially the same half-width (91 cm^{-1} for the plasma-deposited sample, 92 cm^{-1} for the LPCVD one) and no shift towards higher wave numbers (related to the presence of microcrystals[20]) is detected.

It can be concluded that the LPCVD samples are essentially amorphous, and the size of microcrystallites, if any, is below the resolution limit,[21] typical of Raman spectroscopy. A comprehensive comparison between Raman and PDS spectroscopic results on LPCVD films will be the subject of a forthcoming paper.

Concerning the assignment of the $\sim$2100-cm^{-1} mode to hydrogen bonding on inner surfaces of microvoids, the H evolution experiments yield valuable information about the material structure.

For *a*-Si:H films two evolution processes are generally found.[11] At low temperatures ($T<350$ °C) the films are generally permeable to molecular hydrogen. This mechanism is generally explained by considering that the material is a void-rich structure and, upon hydrogen release, the void collapses and a rather compact material is formed.

Beyer *et al.*[22] have explained these results by attributing the low-temperature process to the desorption of H bound to internal surfaces of voids, followed by a diffusion through a network of voids.

The result of Fig. 5 shows a typical H-effusion curve against temperature for a LPCVD sample. This result shows that the low-temperature evolution process is absent in LPCVD material, even if the $\sim$2100-cm^{-1} vibrational peak is detectable. At first sight, the most likely explanation is that the LPCVD *a*-Si:H is a particular kind of void-free material. To support this statement, we have to consider that the deposition temperature T_d is far from typical plasma-deposition ones ($T_d \geq$ 400 °C) so that a kind of compact material can be obtained during the growth. Because of the higher temperatures involved in LPCVD growth, it seems likely that the surface mobility of the deposited atoms is higher than in plasma processes.

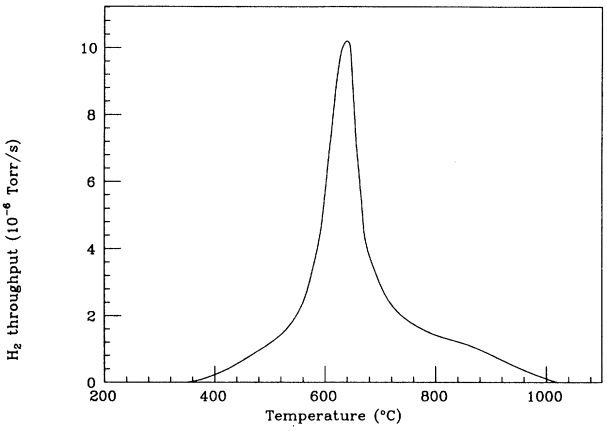

FIG. 5. H-effusion curve for a typical LPCVD sample.

If the void percentage in the LPCVD films is considerably less than in plasma deposited ones, there is no way to attribute the $\sim$2100-cm^{-1} peak to H bound in the internal surface of voids.

As it has been clearly shown in recent works[11,23] the large I(2000 cm^{-1})/I(2100 cm^{-1}) peak ratio in vibrational spectra of sputtered samples could be an effect of the ion bombardment of the film during deposition.

Thus, a "silent" technique, like LPCVD, in which the ion bombardment is practically absent, can provide samples in which the I(2000 cm^{-1})/I(2100 cm^{-1}) peak ratio is considerably smaller. This assumption is in clear agreement with our experimental results.

CONCLUSIONS

We have used the ERDA analysis to calibrate the results obtained by ir vibrational spectra of LPCVD *a*-Si:H. The careful comparison of the two sets of data allows us to evaluate the dipole effective charges for the stretching doublet at 2000–2100 cm^{-1}. The values obtained so far are consistent with the theory and are in good agreement with experimental data obtained on samples grown by means of different deposition techniques. Nevertheless, we have pointed out that the LPCVD material cannot be totally related to the plasma-deposited one, due principally to the higher temperatures used in the process and to the absence of ion bombardment. The study of the structural properties of LPCVD film can be provide an important contribution to the solution of still debated problems. In fact, we have shown that there is no straightforward correspondence between the presence of the $\sim$2100-cm^{-1} vibrational peak and the amount of voids of the material. Thus, the association of the $\sim$2100-cm^{-1} mode with structural and photoelectronic properties of *a*-Si:H is still unclear and needs further study.

[1]*Semiconductors and Semimetals,* edited by P. K. Willardson and A. C. Beer (Academic, New York, 1984), Vol. 21.
[2]M. Cardona, Phys. Status Solidi B **118**, 463 (1983).
[3]H. Shanks, C. J. Fang, L. Ley, M. Cardona, F. J. Demond, and S. Kalbitzer, Phys. Status Solidi B **100**, 43 (1980).
[4]M. H. Brodsky, M. Cardona, and J. J. Cuomo, Phys. Rev. B **16**, 3556 (1977).
[5]H. Wagner and W. Beyer, Solid State Commun. **48**, 585 (1983).
[6]D. Jousee, E. Bustarret, and F. Boulitrop, Solid State Commun. **55**, 485 (1985).
[7]A. H. Mahan, P. Raboisson, and R. Tsu, Appl. Phys. Lett. **50**, 335 (1987).
[8]A. H. Mahan, P. Raboisson, O. L. Williamson, and R. Tsu, Solar Cells **21**, 117 (1987).
[9]A. H. Mahan, P. Menna, and R. Tsu, Appl. Phys. Lett. **51**, 1167 (1987).
[10]S. K. Deb, Thin Solid Films **163**, 75 (1988).
[11]Y. F. Chen, Solid State Commun. **71**, 1127 (1989).
[12]Y. Ashida, Y. Mishima, M. Hirose, and K. Kojima, Jpn. J. Appl. Phys. **23**, L129 (1984).
[13]C. Manfredotti, F. Fizzotti, G. Amato, T. Shamsi, and E. Vittone, *Proceedings of the VIII Photovoltaic Solar Energy Conference, Florence, 1988* (Kluwer, Dordrecht, 1988), p. 902.
[14]G. Amato, G. Benedetto, F. Fizzotti, R. Spagnolo, and C. Manfredotti, Phys. Status Solidi A **119**, 169 (1990).
[15]C. Manfredotti, F. Fizzotti, R. Marchisio, M. Boero, G. Amato, G. Benedetto, and R. Spagnolo, *Proceedings of the IX Photovoltaic Solar Energy Conference, Freiburg, 1989* (Kluwer, Dordrecht, 1989), p. 978.
[16]J. L'Ecuyer, C. Brassard, C. Cardinal, J. Schabbal, L. Déschenes, J. P. Labrie, B. Terrault, J. C. Martel, and R. St. Jacques, Appl. Phys. Lett. **34**, 881 (1976).
[17]D. Campi, and C. Coriasso, Mater. Lett. **7**, 134 (1988).
[18]G. Amato, L. Boarino, F. Fizzotti, and C. Manfredotti, *Amorphous Silicon Technology,* MRS Symposia Proceedings No. 192 (Materials Research Society, Pittsburgh, 1990).
[19]See, e.g., A. Vasicek, *Optics of Thin Films* (North-Holland, Amsterdam, 1960).
[20]R. Tsu, J. Gonzales-Hernandez, S. S. Chao, S. C. Lee, and K. Tanaka, Appl. Phys. Lett. **40**, 534 (1982).
[21]H. Richter, Z. P. Wang, and L. Ley, Solid State Commun. **39**, 625 (1981).
[22]W. Beyer, H. Wagner, J. Non-Cryst. Solids **59&60**, 161 (1983).
[23]S. Oguz, Ph.D. thesis, Harvard University, 1982.